Science Advances

AAAS

advances.sciencemag.org/cgi/content/full/3/11/eaao4795/DC1

Supplementary Materials for

Biomass recycling and Earth's early phosphorus cycle

Michael A. Kipp and Eva E. Stüeken

Published 22 November 2017, *Sci. Adv.* **3**, eaao4795 (2017)
DOI: 10.1126/sciadv.aao4795

This PDF file includes:

Supplementary Text

Electron acceptor compilation

Oxygen

Dissolved oxygen levels were constrained either by proxies that are sensitive to particular levels of dissolved oxygen, or by scaling estimates of atmospheric oxygen levels to dissolved oxygen according to Henry's Law (where pO_2 = 0.21 bar gives an equilibrium concentration of 325 µM).

Atmospheric oxygen levels prior to the Great Oxidation Event (GOE) are constrained by the record of mass-independent fractionation of sulfur isotopes (MIF-S) (*28*). Modeling of this signal imposes an upper limit on pO_2 of less than 10^{-5} PAL (present atmospheric level, *i.e.* ~0.21 bar) (*37*), which equates to 3.25 nM dissolved oxygen in the surface ocean. Oxygen oases containing up to 1-10 µM dissolved oxygen have been proposed for the late Archean (*38*), however, these oases are thought to have been limited in spatial extent and thus the persistence of the MIF-S signature through the Archean can be taken as more representative of global oxygen levels. Even if surface ocean oxygen levels were persistently enriched above equilibrium with atmospheric levels, these concentrations would contribute minimally to global P regeneration (see below).

During the proposed "oxygen overshoot" associated with the GOE (*39*), evidence from iodate concentrations in carbonates (*40*) and selenium isotope fractionations (*41*) suggest that surface ocean oxygen concentrations were at least ~1 µM. While it has been suggested that atmospheric oxygen levels perhaps approached modern values during the "oxygen overshoot" (*39*), there is so far no compelling evidence for such an extreme increase in ambient oxygen. We adopted 5 µM as a conservative estimate of dissolved oxygen from 2.3-2.1 Ga.

After the "oxygen overshoot", pO_2 is thought to have dropped to below 10^{-3} PAL on the basis of unfractionated chromium isotopes in iron formations (*42*) and shales (*43*). This estimate has been challenged by a study that found vanadium depletion in organic-rich shales deposited at 1.4 Ga (*44*), and argued that this reflects suboxic bottom waters under atmospheric oxygen levels of ~4% PAL. In spite of the disagreement about precisely how much oxygen was in the atmosphere and surface ocean during the mid-Proterozoic, the range of values being proposed (0.1-4% PAL) yields minor phosphorus liberation at both the lowest and highest estimates (0.002-0.075 µM P). We adopted the chromium constraint for our preferred model, but note that new evidence for higher mid-Proterozoic oxygen could slightly shift these values. However, it is unlikely that new constraints would significantly change the model output, which consistently shows a small contribution of aerobic respiration to phosphorus recycling (<0.1 µM) before the latest Proterozoic.

It was not until the late Neoproterozoic that atmospheric oxygen began to approach modern levels, and this transition may have been protracted across the early Paleozoic (*45*). We estimated Phanerozoic oxygen levels following the GEOCARBSULF model (*46*). While there remains some dispute as to which model most accurately captures the dynamics of pO_2 over the Phanerozoic, the discrepancies between models do not change our major conclusions.

Nitrate

Marine nitrate concentrations are related to water column redox state, however, the limiting nature of nitrogen as a macronutrient in the marine environment (*2*) prevents nitrate from

building up to substantial levels, even in the oxygen-rich world of the Phanerozoic. Nitrate concentrations in the modern ocean approach ~30 µM (*35*) in regions of nutrient regeneration (*i.e.* nutrient-rich deep waters and upwelling zones), and we therefore consider this as an upper limit on surface ocean nitrate levels from the onset of persistent aerobic nitrogen cycling during the GOE (*47*). Nitrogen isotope data suggest that nitrate did not accumulate in appreciable levels in the oceans during the early- and mid-Archean (*48*), and only transiently during the late Archean (*49, 50*). We therefore considered nitrate to be absent from the oceans prior to 2.7 Ga, at which point it increased to perhaps ~1 µM (globally averaged). Our preferred nitrate abundance curve reaches modern levels during the GOE, after which it diminishes to 10 µM during the mid-Proterozoic, when there is isotopic evidence for nitrate limitation in offshore environments (*51, 52*), and returns to modern levels in the Neoproterozoic. While these estimates remain only qualitatively constrained, the contribution of nitrate respiration to phosphorus liberation is small compared to aerobic respiration and sulfate reduction, and therefore changing between our upper and lower limits does not impact our ultimate conclusions.

Manganese

Manganese (Mn) has multiple oxidation states, and can serve as a strong oxidizing agent in the natural environment. In aqueous environments, Mn typically occupies the +II or +IV oxidation state, the latter of which is insoluble. As such, the secular increase in oxygen content of Earth's surface environment has likely been accompanied by a decline in the Mn content of the ocean (*53*).

Dissolved Mn^{+II} is present at a concentration of ~1 nM in modern seawater (*54, 55*), and the dominant oxidized Mn species (particulate MnO_2) has a correspondingly short residence time in seawater due to its relatively rapid settling out of the water column (*56*). As such, Mn does not significantly impact organic remineralization or P liberation on a global scale [although in local environments it can play a substantial role (*57*)]. While empirical constraints on Precambrian Mn concentrations are lacking, modeling work (*53*) has estimated that concentrations were slightly higher than modern in the more reducing oceans of the Archean and Proterozoic. We therefore adopted the estimate of 1-10 nM (*52*) for Precambrian levels, with 10 nM as our preferred value. At these levels, Mn remains a negligible contributor to global P liberation.

Iron

The concentration of dissolved iron and persistence of ferruginous conditions in the Precambrian has long been the subject of geochemical scrutiny, however, precise empirical constraints on iron concentrations remain difficult to obtain. Holland estimated that Archean and early Paleoproterozoic ferrous iron concentrations were 40-120 µM (*30, 26, 58*). This range corresponds to the concentration of ferrous iron at saturation with respect to siderite and calcite, assuming a range of calcium concentrations similar to Phanerozoic values. The absence of considerable siderite in Archean carbonates would seem to suggest that ferrous iron concentrations were well below this value. If calcium concentrations were in fact higher in the Archean, as recent models have considered (*5*), and atmospheric CO_2 levels were considerably higher than modern (*59*), then the corresponding iron concentrations at siderite and calcite saturation could have been even lower. Still, we adopted the higher end of this range as our preferred value in order to remain conservative in our calculations.

Recent work has introduced additional complexity to the picture of Archean seawater Fe levels. Some have challenged these constraints on the basis that precipitation kinetics are much slower for siderite than for calcite (*60*); in order to achieve similar precipitation rates for calcite and siderite, some experiments have shown that the saturation state of siderite needed to be ~3 orders of magnitude higher than calcite (*61*). The threshold for ferrous iron concentrations imposed by the lack of considerable siderite in Archean carbonates may thus be much higher than estimated above. However, siderite precipitation may still have played a role in determining dissolved iron concentrations. The abiotic precipitation of calcite from seawater tends to occur when the degree of supersaturation exceeds ~20 (*62*), whereas siderite tends to require ~50 times supersaturation (*63*). Recent workers have compared the upper limits on ferrous iron concentrations imposed by kinetically-inhibited siderite precipitation to upper limits imposed by reduced iron-silicate minerals (*25, 64*). This work has shown that requiring ~60 times supersaturation for siderite formation generates approximately the same upper limit as would be imposed by the precipitation of greenalite from seawater, which is ~1 mM (*25*). However, more recent modeling has suggested that "green rust" – a metastable, ferrous-ferric mineral – could have been precipitated more efficiently from Archean seawater than greenalite (*64*), perhaps implying that ferrous iron concentrations could have been well below the 1 mM upper limit proposed based on greenalite solubility. In either case, the reported discovery of primary iron-silicate phases in BIFs would seem to support the notion that ferrous minerals did in fact precipitate from seawater in the Archean and contribute to BIF deposition in at least some environments (*65, 66*). The emerging view now holds that there may have been differences in primary mineralogy among BIFs deposited in deeper versus shallower environments (*67*). In order to allow for all

possibilities in our model scenarios, we have generated our Archean model outputs as a function of iron availability ranging up to the 1 mM greenalite constraint.

Assuming that all of this ferrous iron could be upwelled onto continental shelves and quantitatively oxidized to ferric iron, this can be used as an upper limit on ferric iron concentrations (*68*). It is important to note that phototrophic oxidation of ferrous iron does not add to the net supply of oxidants for P recycling, because phototrophic organisms consume P at first instance. In principle, the same is true for chemotrophic Fe^{2+} oxidation with O_2 or NO_3^-. However, the O_2 and NO_3^- concentrations that we used in our model (Section 2.1) are equilibrium values after reaction with Fe^{2+}. The Fe^{3+} generated in those reactions can therefore enter the equation. Our approach of allowing all dissolved Fe^{2+} to convert to Fe^{3+} is highly conservative. Abiotic photochemical Fe^{2+} oxidation is presumably of minor importance (*69*), though again this pathway is accounted for in the equilibrium concentrations used in our calculations. To constrain ferric iron concentrations after the cessation of substantial BIF deposition at 1.8 Ga, we follow the model of Saito et al. (*53*), which estimated ~100 nM levels for the mid-Proterozoic and ~1 nM levels for the Phanerozoic, which is consistent with observations in the modern ocean (*52*).

Sulfate

Sulfate is a major ion in modern seawater, with a concentration of ~28 mM. Paleo-concentrations of sulfate in the surface ocean are estimated primarily using sulfur isotope geochemistry, including multiple sulfur isotope systematics and the rate of change of sulfur isotope values along stratigraphic profiles. These studies have generated a record of Phanerozoic sulfate

concentrations that fluctuate in the mM range (*70*), as well as several constraints from the Precambrian.

Early constraints on Archean sulfate concentrations were derived from the observation of minimal sulfur isotope fractionation during sulfate reduction in cultures with sulfate concentrations <200 µM (*71*). The muted isotopic variability of sulfur in sedimentary sulfides prior to the GOE is thus compelling evidence for surface ocean sulfate concentrations below this threshold (*72*). However, new insights into sulfur isotope systematics have successively pushed this limit lower. Data from Neoarchean volcanogenic massive sulfides were used to generate an estimate of ~80 µM sulfate at this time, with a probability distribution encompassing 0 µM to 175 µM (*73*). More recently, studies of modern analog environments and new Neoarchean sulfur isotope stratigraphy have established an upper limit of <10 µM and a maximum likelihood estimate of 2.5 µM (*23*, *24*) which we adopted for our calculations.

During the GOE, it has been argued that the marine sulfate reservoir expanded coincident with the proposed "oxygen overshoot" event (*74–76*), perhaps reaching near-modern levels (5-20 mM) before contracting in the aftermath of the GOE. In the mid-Proterozoic, estimates range from 100-350 µM (*77*) to 1-4 mM (*78*). We adopted a value of 10 mM during the GOE, and subsequent return to 350 µM in the mid-Proterozoic. From the mid-Proterozoic onward, sulfate levels steadily increase to ~2 mM in the later Proterozoic, and higher in the Phanerozoic. While there is not yet a clear consensus regarding a preferred secular trend, we considered the entire range of the most recent estimates to derive our uncertainty interval.

Soluble vs. insoluble electron acceptors

Unlike the other electron acceptors in our calculation, both Mn and Fe are less soluble in their oxidized states than reduced states (*79*). For this reason, their cycling within the ocean system is considerably different. Both Mn and Fe are transported to the ocean by fluvial, aeolian, and hydrothermal processes (*56, 80, 81*), with fluvial inputs dominating the modern flux (*14, 56*). Upon reaching the ocean, Mn and Fe oxides have a short residence time. It is estimated that ~95% of riverine Fe and ~25-45% of riverine Mn are oxidized into reactive particulates during fluvial transport and estuarine mixing (*82, 83*). Abundance profiles moving offshore show relatively quick removal of Fe and Mn from the water column and settling into sediments (*56*). Thus, while these oxidized particulates are highly reactive toward organic matter, their oxidative capacity is spatially limited to sediments near riverine sources. Furthermore, as the dissolved phases tend to flocculate upon oxidation (*83*), the oxidizing potential becomes restricted to particle surfaces, meaning that the net oxidative capacity is lower than would be predicted by bulk concentrations. In the Precambrian, the hydrothermal Fe and Mn sources may have dominated (*84*), and oxidation may have occurred primarily in upwelling zones, perhaps represented by banded iron formations on continental shelves (*85*). But in any case, the observations from modern rivers illustrate the short reach of iron oxides as biomass oxidants.

In our calculations, we have treated insoluble and soluble electron acceptors equally for the sake of simplicity and in order to generate a conservative upper limit on potential P recycling. In reality, an accurate consideration of net organic remineralization achieved by Fe and Mn would require more detailed chemical modeling than is the goal of this calculation. However, because we have operated on the conservative assumption that all dissolved Fe and Mn in the ocean

system could be oxidized, and quantitatively used to oxidize organic matter, the net amount of P recycling we are attributed to these electron acceptors is likely an over-estimate of the real amount. Thus, we find this treatment of insoluble electron acceptors to be sufficient for the purposes of our calculations (which is to demonstrate the maximum possible amount of P recycling in the Precambrian oceans), despite being an over-simplification of the operating chemistry.

Constraining the contribution of organic disproportionation reactions

When the supply of electron acceptors becomes depleted, biomass can continue to be degraded through organic disproportionation reactions that do not utilize dissolved electron acceptors. Instead, these reactions can split organic molecules with no net change in oxidation state. A common example is heterotrophic methanogenesis, with the net reaction

$$2\,CH_2O \rightarrow\ CH_4 + CO_2 \qquad (3)$$

Additionally, fermentative reactions can split organic matter and produce hydrogen in the process

$$2\,CH_2O + 2\,H_2O \rightarrow\ 2\,CO_2 + 4\,H_2 \qquad (4)$$

which can then be utilized to fuel autotrophic methanogenesis

$$CO_2 + 4\,H_2 \rightarrow\ CH_4 + 2\,H_2O \qquad (5)$$

All of these reactions can contribute to P liberation, and are hereafter referred to simply as "methanogenesis" since the net outcome of the proliferation of these metabolic pathways is the production of biogenic methane.

In the modern ocean, methanogenesis is not thermodynamically favorable in the water column (*17*), but can become significant at depth in sediments, particularly where settling rates of organic material are high. However, its spatial restriction and limited supply of substrate make methanogenesis a minor player in the recycling of P within the modern ocean. Canfield estimated that the net contribution of methanogenesis to organic remineralization is 5-10 times less than that of sulfate reduction, which itself sustains only 8-14% of total biomass recycling (*86*). Scaling this output to modern P recycling rates generates a modern methanogenic P recycling flux of 0.008-0.028 μM, with a mean of 0.018 μM.

In order to scale this value for the Precambrian, we compare modern methanogenesis rates in marine sediments [20 Tmol/yr (*17*)] to proposed values for the late Archean [96 Tmoly/yr (*18*)], which is thought to have been a time of vigorous methanogenesis on the basis of extreme depletion in the carbon isotopic composition of organic matter in late Archean sedimentary rocks (Fig. 1B). Thus, by scaling to this interval, we are making the most conservative assumption regarding the possible impact of methanogenesis on P recycling. Multiplying the modern value (0.018 μM) by a scaling factor of 4.8 (96/20) gives a P regeneration flux of 0.086 μM. This is our upper limit on Precambrian P recycling by methanogenesis, and we conservatively apply this value to the entirety of the Precambrian, even though the late Archean was likely a time of

exceptionally vigorous methane production. Furthermore, if the higher biogenic methane flux in the late Archean in fact came predominantly from autotrophic methanogenesis that utilized a higher H_2 flux than is present on the modern Earth, we would be considerably over-estimating the methanogenic contribution since most autotrophic methanogenesis on the modern Earth is fueled by fermentation-derived H_2 (Reaction 4), which requires biomass degradation for its production. In light of this assessment, it seems that methanogenesis could have had a non-negligible impact on P recycling in the Archean, but likely could not have overcome the inhibition of P recycling at this time.

Interpreting the proxy record

Testing the limited-recycling model will require careful interrogation of the sedimentary record. To date, most empirical studies of P in ancient marine sedimentary rocks have focused on iron-oxide rich sedimentary rocks (*3–5*); more recently siliciclastic sedimentary rocks have been targeted as well (*6*). These records have both been used to argue for low P levels in the Precambrian (*3*, *5*, *6*), though extracting quantitative estimates of P levels has remained contentious (*7, 87*). Here we consider the Fe-oxide and shale records through the lens of the limited-recycling model.

By carefully considering the environmental chemistry in the depositional sites, P/Fe ratios in iron-rich sedimentary rocks can be used to generate estimates of dissolved P levels at the time of deposition (*88, 89*). The first such work in a Precambrian context focused on Archean and late Paleoproterozoic banded iron formations (BIFs), with results implying significantly lower marine P levels (*3*). While this interpretation hinges on several assumptions about paleo-seawater

composition (*7*), the latest modeling and experimental work has suggested that the original interpretation of low P remains valid (*5*).

Unfortunately, the record of BIFs is discontinuous, and is tied to the very chemical conditions that are thought to be conducive to low P levels (anoxic oceans with possibly limited biomass recycling, as well as potentially vigorous Fe-scavenging). Thus, it may be unsurprising that these archives persistently generate estimates of low marine P levels. The BIF record compellingly shows that P was fairly low in the late Archean and in the aftermath of the "oxygen overshoot" of the Paleoproterozoic [after ~2.06 Ga]. Our model is entirely consistent with these observations, and in fact invokes higher P in the gaps of the BIF record, *i.e.* during oxygen overshoot [~2.32-2.06 Ga (*39*)] and in the later Proterozoic. Thus, the BIF record may not be a suitable place to test the limited-recycling model.

In search of a more ubiquitous lithology, Reinhard et al. (*6*) assembled a database of P abundances in marginal marine siliciclastic sedimentary rocks (fig. S3). The record of these sediments is much more continuous, even despite the generally sparse nature of the Precambrian rock record. The interpretation of this dataset favored by Reinhard et al. (*6*) was that the significant increase in P concentrations in these sedimentary archives in the latest Proterozoic coincided with the termination of effective Fe-scavenging, which was limiting the size of the P reservoir throughout most of the Precambrian. Alternatively, it is possible that at times, the limited P enrichment in these rocks is a result of limited recycling of biomass-bound P. There is a small, but statistically significant spike in the P content of marine sediments during the GOE (fig. S3), as well as a decrease in C:P ratios (fig. S3). This could be a result of more oxidizing

conditions in the oceans, with greater rates of P recycling, a larger P reservoir, and thus greater contribution of authigenic P to the total P content of marine sedimentary rocks, causing C:P ratios to be lower than "Redfield" values. The return to lower P levels and higher C:P ratios in the aftermath of the GOE may be signal of a return to low-P conditions, although whether this is due to Fe-scavenging or limited recycling is not discernible with these data alone. Given the available data, though, the changes seen across the GOE seem indicative of an over-arching redox control of P cycle behavior.

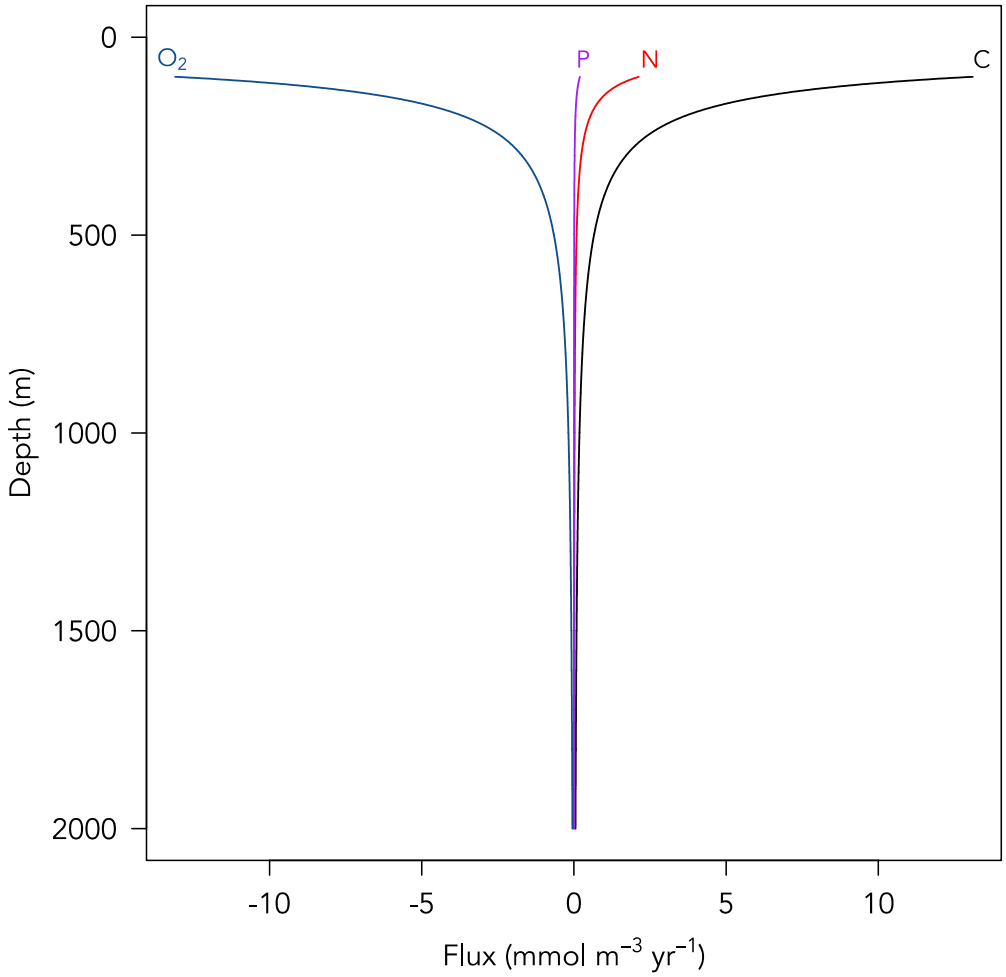

fig. S1. Estimated annual fluxes of C, N, P, and O_2 consumption as a function of depth. Modified after Figure 6 in (*9*). C and N curves were derived from normalized power functions used to fit data obtained in (*9*). P curve was generated by stoichiometrically converting the C curve based on published estimate of preferential release coefficient (*12*). O_2 curve was generated assuming 1:1 O_2:C net stoichiometry of aerobic respiration (*16*).

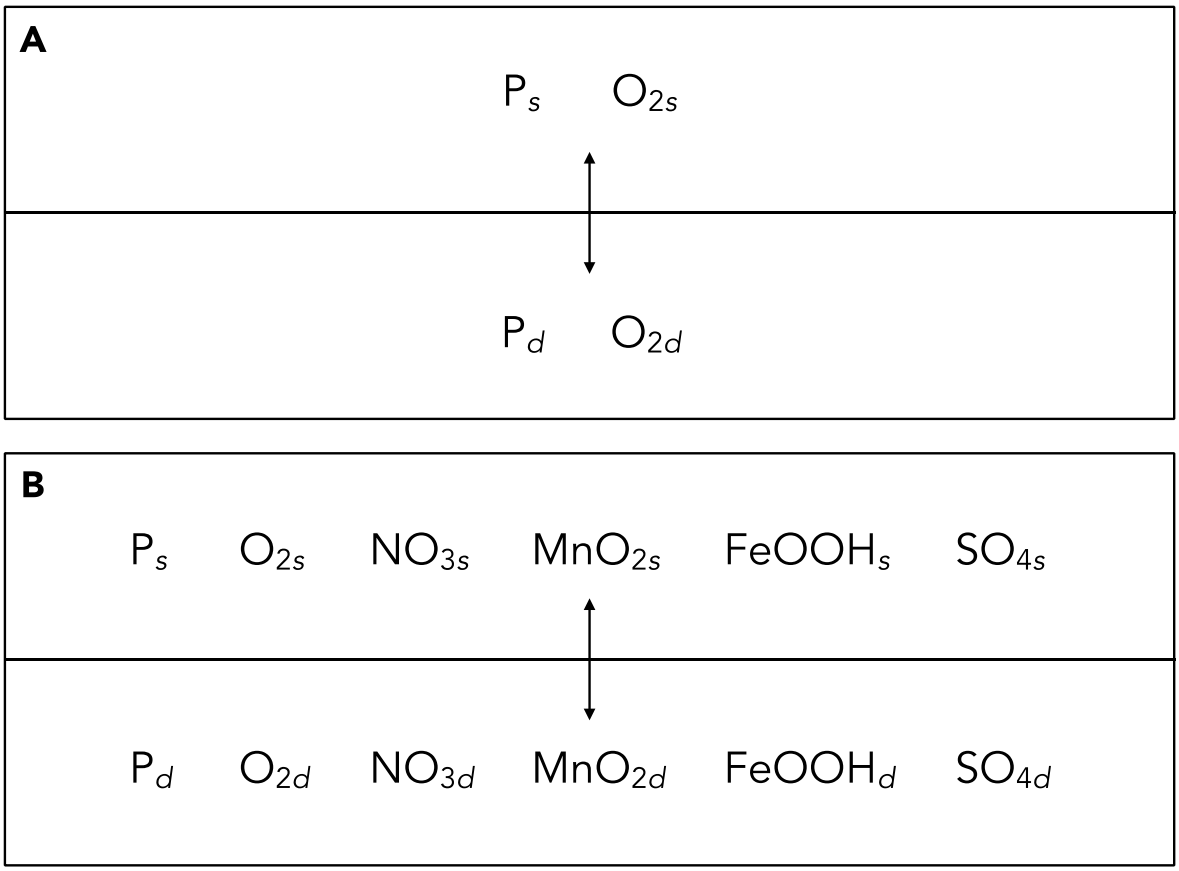

fig. S2. Box model schematic. (**A**) shows O_2-only model, from (*12*); (**B**) shows modified Precambrian model including anaerobic oxidation pathways.

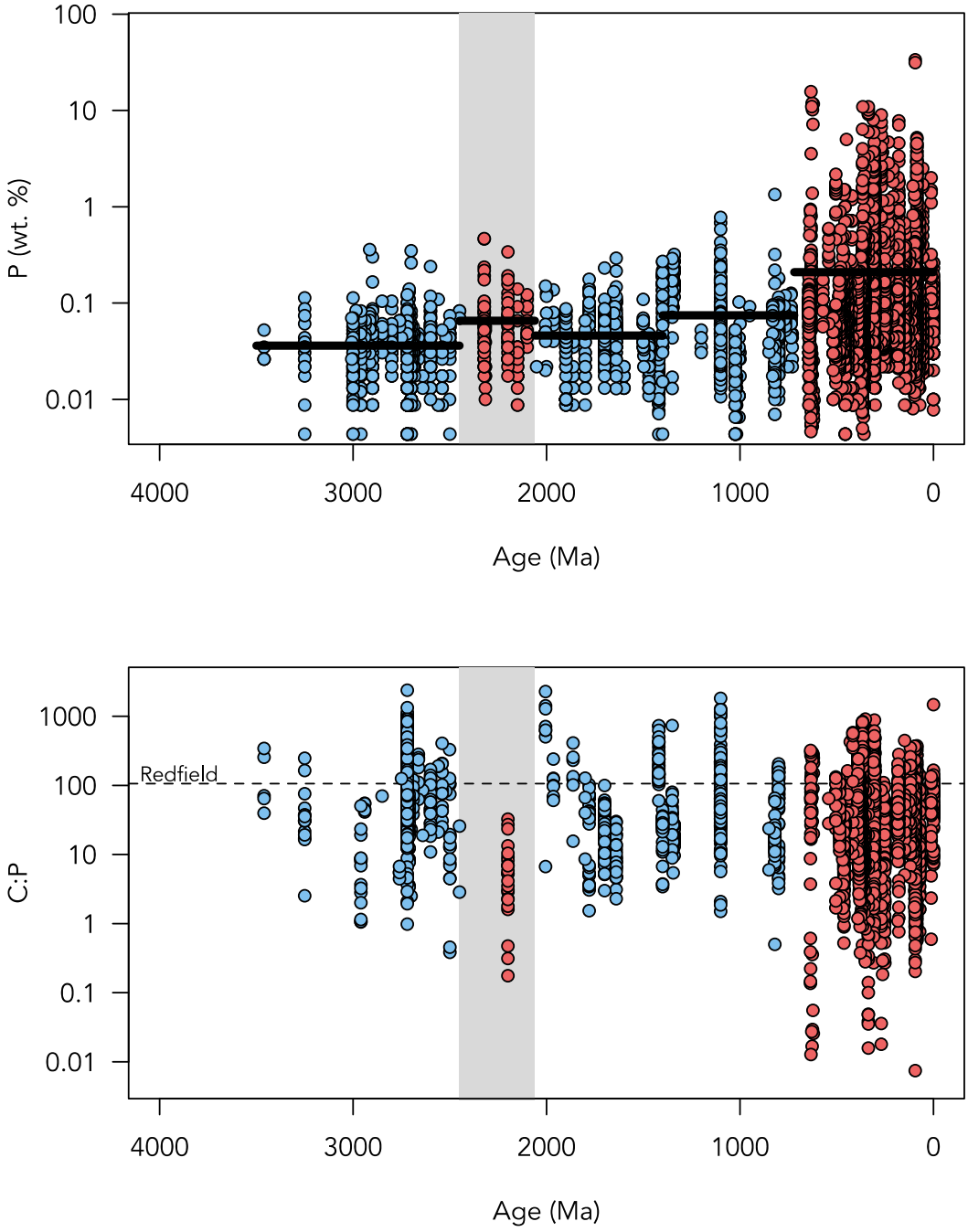

fig. S3. P concentrations and organic C/P ratios in marginal marine siliciclastic sedimentary rocks. Black bars in top panel show average values within age bins (pre-GOE, >2.45 Ga; GOE, 2.45-2.06 Ga; post-GOE, 2.06-1.4 Ga; late Proterozoic, 1.4-0.72 Ga; modern, <0.72 Ga). Grey shaded regions mark the "oxygen overshoot", where our model predicts higher marine P levels. Dotted line in bottom panel shows modern Redfield C:P ratio.